



Design and Analysis of PTO Shaft for a Fighter Jet Aircraft Considering Gyroscopic Effects

¹Ramakrishnaprasad U Pait, ²S B Kandagalty, ³Rajath Rao

¹Department of Mechanical Engineering, NMAM Institute of Technology, Nitte – 574110, India

²Principle Research Scientist, Department of Aerospace Engineering, IISc, Bangalore – 560012

³Assistant Professor, Department of Mechanical Engineering, NMAM Institute of Technology, Nitte – 574110, India

Abstract

This paper shows an approach in designing a high-speed PTO (Power Take-Off) Shaft assembly system, which acts as a mechanical link between the engine and AMAD (Aircraft Mounted Accessory Drive), considering the gyroscopic effects when analyzing the static and dynamic behavior. Gyroscopic effect is one of the various parameters which effect the operation of the PTO system. Failure of this shaft will cut off all the hydraulics and other controls to the aircraft operation which can further lead to the loss of aircraft itself. FEA Tools, such as ANSYS is used for performing the desired analysis. An effort has been made to meet-up the critical speed margin, within which the PTO System operates. The system is also designed to counter the parallel and angular misalignments caused due to vibration or thermal expansion with the help of high-speed flexible coupling.

Keywords: Rotor Dynamics, PTO Shaft, Flexible Coupling, Critical Speeds.

1. Introduction

Rotor dynamics is a field under mechanics, mainly deals with the vibration of rotating structures. Some of the examples under rotor dynamic structure are wind turbine, marine propulsion system, turbo machinery, jet engines etc. In recent days of technological advancement, the study of rotor dynamics has gained more importance with in aerospace industry. One of such rotating part in the aerospace sector is the PTO shaft system, which serves the purpose of transmitting power from engine to AMAD. Figure 1 shows a typical sketch for PTO Shaft assembly.

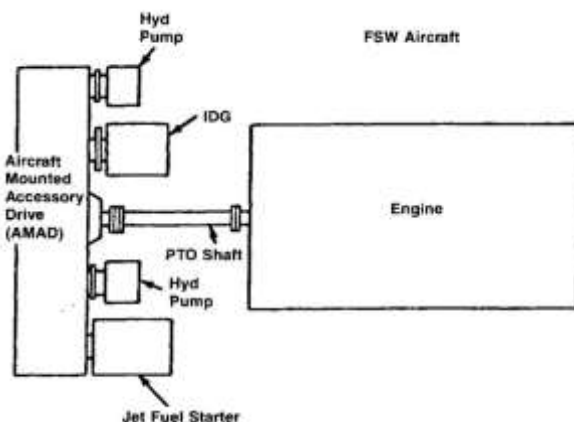


Figure 1: Engine, PTO Shaft and AMAD Assembly

Current design trends for rotating equipment aim to increase the efficiency and reduce overall weight as to achieve higher operating speeds. Vibration analysis is essential in the design and analysis of rotating machinery. The majority of vibrations are

caused by rotation related sources, normally imbalance. Consequently, the forces are synchronous to the rotational speed. Thus, forced vibration analysis is fundamental in the design and analysis of rotating machinery. The two most commonly used methods of forced frequency analysis are the finite element, or transfer matrix method. However, since certain effects (including gyroscopic effect, centrifugal stiffening, and fluid bearings) are dependent on the rotational speed the methods require computational assembly and inversion of large matrices at each frequency step. This is computationally expensive and inefficient however with the advances in modern computing speed it is rapidly becoming less of a problem.

In the analysis of system involving rotors spinning with high velocity, it becomes essential to include the effect of gyroscopic moment for the critical speed analysis. This paper shows the effects of the same on different modes and natural frequency of the PTO rotating system.

2. Brief Background

2.1 Rotor Dynamics

Rotor dynamics is a branch of applied mechanics which deals with study of rotating structures. This includes study in the performance behavior of jet engines and steam turbines to auto engines and computer disk storage.

The simplest form of rotor dynamic system consists of its shafts supported on its ends with the help of bearings. Furthermore, this shaft can have more number of bearings fixed to the support or can be loaded with one to 'N' number of disks. With increase in speed the induced vibration also increases to reach a maximum at its critical speed, when it matches up with system natural frequency.

2.2 Modes of Rotation and Whirling of Shaft

In rotor dynamics, importance is given to first two modes of rotation. First one being the cylindrical mode, is apparent at lower rotating speeds. Their frequencies are quite close to the non-rotating ones. To visualize how rotor is moving, imagine swinging a rope around. The path traced by it can more or less will give us an idea of cylindrical mode.

Second one is the conical mode; whose frequencies lie slightly higher than the cylindrical mode. To visualize how rotor is moving, imagine holding a rod stationary in the center and moving it so that its ends trace out two circles. Figure 2 shows a sketch of both cylindrical and conical mode.

When we consider the types of whirl conditions, again there are two types. At first is the condition where in whirl motion is same as the rotation direction, it's called as forward whirl and in case of backward whirl, the whirl and direction of rotation oppose each other. When we perform analysis on high speed structure, under conical mode, we can see that the frequencies of this mode do change over at higher speeds. The backward mode drops in frequency and the forward mode frequency increases slightly. This is due to gyroscopic effect on the system. Figure 3 shows a sketch of forward and backward whirl condition.

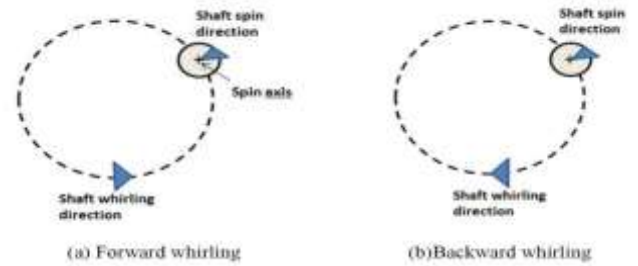


Figure 3: Forward and Backward Whirl Condition.

2.3 Gyroscopic Effect

It is one of the many dynamic phenomenon which a rotating structure undergoes. In brief, the gyroscopic effect comes into picture at higher speeds only. The overall stiffness of the system changes with the change in rotating speeds, hence changing the natural frequency of the system.

Firstly, consider forward whirl, as the rotating speed increases, the gyroscopic effects essentially act as the spring with increasing stiffness thereby increasing the natural frequency. In case of backward whirl, the case is opposite and gyroscopic effect tends to soften the system stiffness, hence a decrease in natural frequency. The equation of motion which considers gyroscopic effect into account is shown in Eq. (1). It describes the motion of an axially symmetric rotor, which is rotating at a constant spin speed Ω about its spin axis. This equation is similar to the general dynamic equation except it is accompanied with skew-symmetric gyroscopic matrix, $[C_{gyro}]$ and skew symmetric circulatory matrix $[H]$. The gyroscopic and circulatory matrices are greatly influenced by the rotational velocity Ω , which when tends to zero, the skew symmetric terms present in the equation above vanish and represent ordinary stand still structure.

The gyroscopic matrix contains inertial terms that are derived from kinetic energy due to gyroscopic moments acting on the rotating parts of the machine. If this equation is described in rotating reference frame, this gyroscopic matrix also contains Coriolis acceleration. The circulatory matrix is contributed mainly from internal damping of rotating element.

$$[M] \{\ddot{u}\} + ([C] + \Omega [C_{gyro}]) \{\dot{u}\} + ([K] + [H]) \{u\} = \{f\} \quad (1)$$

The net result with the inclusion of gyroscopic effect is the stiffening of the softening effect. Figure 4 shows a typical Campbell diagram to show the effect of gyroscopic moment on the natural frequency of the rotating system.

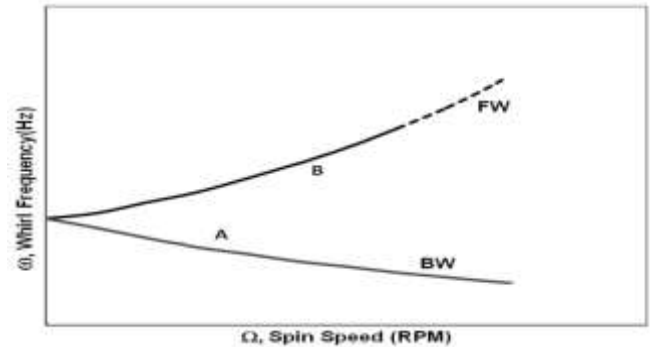


Figure 4: Campbell Diagram.

2.4 Misalignment

Shaft misalignment is generally accepted as one of the major sources of vibration in rotating machinery.

Such misalignment introduces static and dynamic forces which can result in damage to the machinery and can result in failure. Additional undesirable effects such as excessive noise and increased power consumption have also been reported.

It is impossible in practice to achieve perfect alignment between the driving and driven shafts and it is for this reason that the flexible inter-connections are introduced with the aim of minimizing misalignment imposed lateral forces while ensuring the efficient torque transmission. These flexible interconnections include flange type coupling, gear type coupling, disc coupling (single or stacked), diaphragm coupling

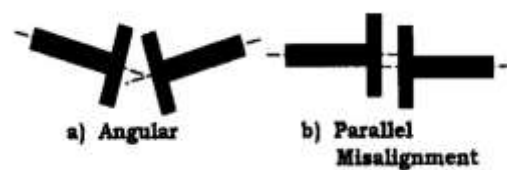


Figure 5: Angular and Parallel Misalignments.

etc. When the rotational axes of drive and the driven shafts are non-coincident at the point of coupling the shafts are considered to be misaligned. Shaft misalignment is usually defined in terms of angular and parallel components. Figure 5 shows these two types of misalignment in a sketch.

2.5 Flexible Diaphragm Coupling

The PTO shaft system analysed in this paper uses the Flexible Contoured Type coupling in order to overcome the problem of misalignment. The contoured type of coupling discs are very flexible members and is used for high power and speeds.

It is designed to a specific shape between the hub and the rim such that the material is utilized efficiently meetup required design aspect. All relative movement occurs as flexing in the countered section there by eliminating the need for lubrication. These flexible elements can also be used in series to provide high

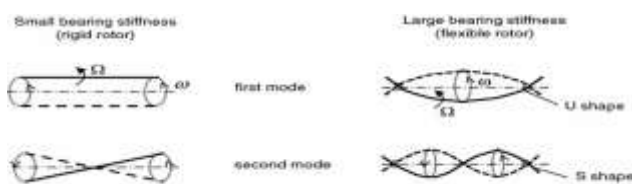


Figure 2: Cylindrical and Conical mode of vibration

misalignment corrections without increasing the stress on any one of the existing elements. The reason for selecting this type of flange is shown in the Table 1.

Table 1: Comparison Chart for Flexible Coupling.

FUNCTION	MECHANICALLY FLEXIBLE				ELASTOMERIC				METALLIC MEMBRANE			
	FLANGE	FLANGE	FLANGE	FLANGE	FLANGE	FLANGE	FLANGE	FLANGE	FLANGE	FLANGE	FLANGE	FLANGE
MAXIMUM PERMISSIBLE TORQUE (Nm)	4000	3000	1200	220	450	3000	40	1700	1000	120	700	700
MAXIMUM SPEED (rpm)	12000	14000	20000	6000	4000	2000	6000	2000	20000	20000	20000	20000
MAXIMUM DEFLECTION (mm)	300	300	300	250	300	300	250	400	270	300	300	300
MAXIMUM MISALIGNMENT (°)	1.1	1.1	0.25	2	0.2	2	1	1	0.4	0.1	0.1	0.1
TORSIONAL STIFFNESS (Nm/mm)	100	100	100	1.0	0.2	0.2	0.2	0.2	100	100	100	100
MAX. TORSION	1000	1000	1000	100000	100000	100000	100000	100000	100000	100000	100000	100000
MAXIMUM WEIGHT (kg)	100	100	100	100	100	100	100	100	100	100	100	100
MAXIMUM PRICE	100	100	100	100	100	100	100	100	100	100	100	100
MAXIMUM LIFE (hrs)	10000	10000	10000	10000	10000	10000	10000	10000	10000	10000	10000	10000
MAXIMUM EFFICIENCY (%)	98	98	98	98	98	98	98	98	98	98	98	98
MAXIMUM VIBRATION	100	100	100	100	100	100	100	100	100	100	100	100
MAXIMUM NOISE (dB)	100	100	100	100	100	100	100	100	100	100	100	100
MAXIMUM MAINTENANCE	100	100	100	100	100	100	100	100	100	100	100	100
MAXIMUM RELIABILITY	100	100	100	100	100	100	100	100	100	100	100	100
MAXIMUM WEIGHT	100	100	100	100	100	100	100	100	100	100	100	100
MAXIMUM PRICE	100	100	100	100	100	100	100	100	100	100	100	100
MAXIMUM LIFE	100	100	100	100	100	100	100	100	100	100	100	100

As it is evident in the given table, the coupling can handle the various operational extremities which it can undergo while under operation. Figure 6 and Figure 7 shows a cross-section of Flexible Diaphragm Coupling Plate.

3. Design Requirements

The initial step was to establish the design requirements for the desired model. Table 2 shows the boundary conditions within which the design was to be completed.

Table 2: Design Requirements.

Sl No.	Design Requirements	
	Parameters	Values
1	Maximum allowable length	490 ± 1 mm
2	Range of Diameter for Shaft	40 – 60 mm
3	Range of Thickness for Shaft	1 – 4 mm
4	Operating Speed of the Shaft	10000 – 20000 rpm
5	Allowable Lateral Deflection	± 5 mm
6	Maximum Applicable Torque	90 Nm
7	Maximum Number of Diaphragm Pairs Allowed	4 numbers on each side.

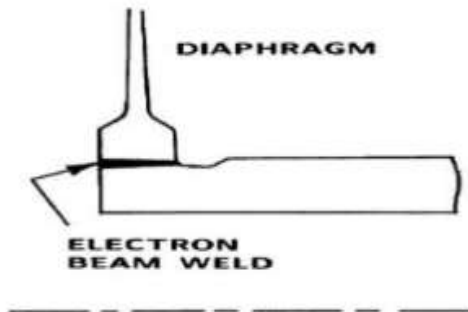


Figure 6: Diaphragm plate fixed to the Hub.

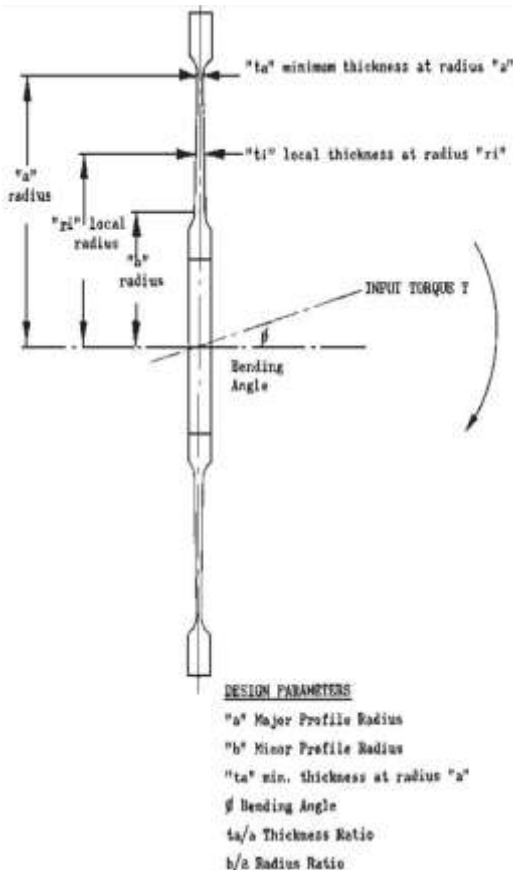


Figure 7: Cross-Sectional view of a Flexible Diaphragm Coupling Plate.

According to this condition proper material for each of the parts, their dimensions, number of diaphragm pairs to be used should be finalized based on the analysis. Since maximum torque on the system is experienced while initial stages of driving the engine, this factor was also to be considered.

4. Initial Design

It was established that out of many materials available in the market, 4340 VAC AMS 6414 for diaphragm plates and AISI 4340 for other components were finalized. This was done based on the proposed design conditions, which also proved good enough for the overall performance. The material properties are listed in the Table 3 and Table 4 for the reference.

Since material were finalized, a basic design was made by considering two pairs of diaphragm on each side and taking the shaft diameter and thickness being varied from 40 - 60 mm (in the steps of 5mm) and 1 – 4 mm (in the steps of 0.5mm) respectively, and for overall system length of 491 mm. Every combination for diameter and thickness were subjected to critical speed analysis. From the data obtained, it was observed that, for the combination of 60mm diameter and 4 mm thickness of shaft, the critical speeds were at their best behavior.

Now taking the same shaft specifications, critical speed analysis was performed by changing number of diaphragm pairs while keeping overall length of the system constant at 491 mm by changing the shaft length accordingly.

From the critical speed results as shown in the Table 5, it is evident that the system with 4 pairs of diaphragm is the best possible configuration. Also, the critical speed for 5th mode falls just above the 20000 RPM range, which is outside the critical speed margin. Figure 8 and Figure 9 shows the overall assembly and split open figure of the PTO shaft system with 4 pairs of diaphragms.

5. Analysis and Results

After finishing the PTO shaft system design, final task was to meet up the remaining design requirements, such as its flexural ability and overall strength. ANSYS which happens to be a FEA tool was used and the system was subjected to static structural analysis.

At first, in order to satisfy system's flexural needs, it was subjected to a lateral force of 460 N at one end of the flange while fixing the other end. The results showed us that the system was able to handle the maximum deformation of 16.046 mm while

undergoing a maximum stress of 859.26 MPa in the diaphragm rim. Then the same system was subjected to a torque of 90 Nm t one of its flange ends while fixing the other end. Upon finishing the analysis, the results indicated a maximum stress of 50.15 MPa at diaphragm.

Both of these loading conditions do not affect the integrity of the system, as maximum yield strength for the diaphragm materials was 862 MPa. Below Figures 10, 11, 12, 13 and 14 shows the various load conditions and results obtained from ANSYS.



Figure 8: Assembled View of PTO Shaft



Figure 9: Section View of PTO Shaft Assembly

Table 3: Material Properties of 4340 VAC AMS 6414.

Sl No.	Material Properties	
	Parameters	Values
1	Density	7872 Kg/m ³
2	Modulus of Elasticity	205 GPa
3	Ultimate Tensile Strength	1279 MPa
4	Yield Strength	862 Mpa
5	Poisson's Ratio	0.3

Table 4: Material Properties of AISI 4340.

Sl No.	Material Properties	
	Parameters	Values
1	Density	7850 Kg/m ³
2	Modulus of Elasticity	205 GPa
3	Ultimate Tensile Strength	1110 MPa
4	Yield Strength	710 MPa
5	Poisson's Ratio	0.29

Table 5: Critical Speed Data for 4 Pairs of Diaphragm

Modes of Vibration	Critical Speeds (in RPM)			
	1 Pair	2 Pair	3 Pair	4 Pair
1	1453.9	1036.5	840.28	727.05
2	1489.2	1070.6	856.35	741.16
3	16177	11416	9082.7	7793.3
4	None	18896	13875	10945

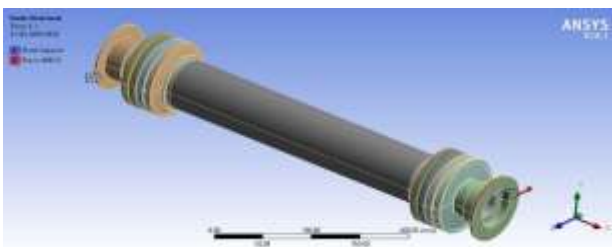


Figure 10: PTO Shaft Lateral Loading Condition

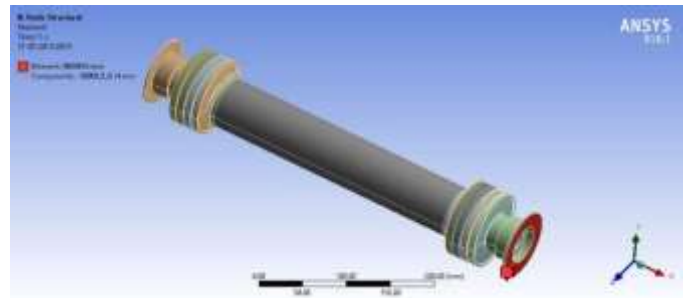


Figure 11: PTO Shaft Torque Loading Condition

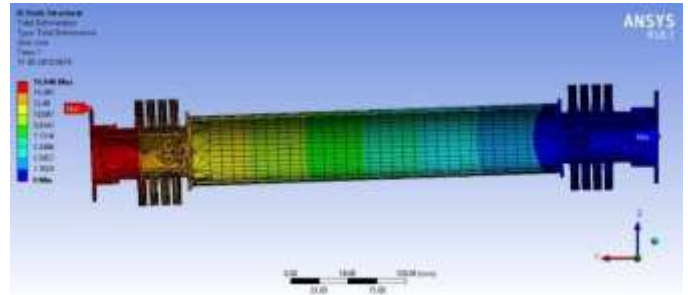


Figure 12: Overall Deflection for Lateral Loading Condition

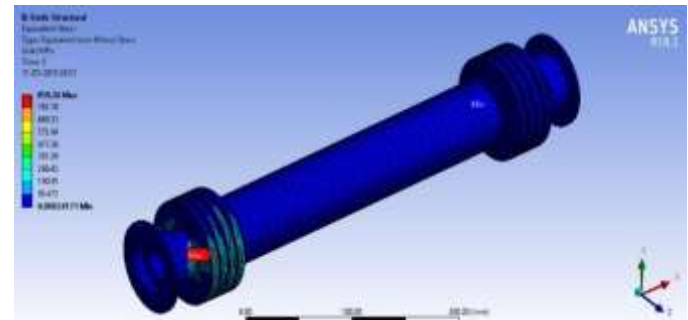


Figure 13: Maximum Stress for Lateral Loading Condition

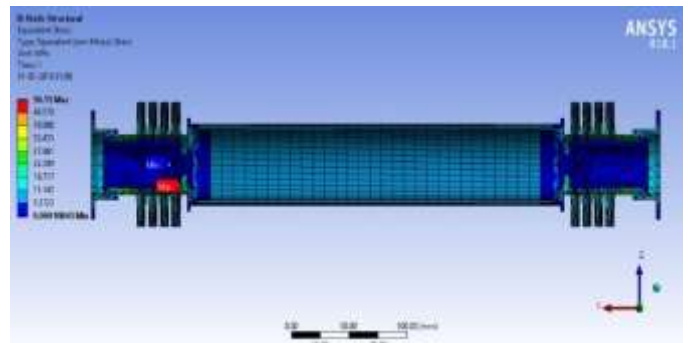


Figure 14: Maximum Stress for Torque Loading Condition

6. Conclusion

A proper PTO shaft system was designed based on the initial conditions right down to every single component. The major concerns were its critical speed margin, flexural ability and overall strength.

Multiple combinations for shaft and diaphragm were subjected to critical speed analysis and satisfactory results were obtained, wherein these critical speeds do not overlap with operating speeds. Also, the system was subjected to various loading conditions and results confirm that the minimum required flexural ability and overall strength of the system.

Furthermore, these results can be enhanced by subjecting overall system to dynamic analysis to obtain higher accuracy.

References

- [1] Rao, J. S., 1996, Rotor dynamics, New Age International Publishers.
- [2] Kandil, M. A., 2004, "On rotor internal damping instability", Doctoral thesis, Department of Mechanical Engineering, Imperial College of London.
- [3] Dickmen, E., 2010, "Multiphysical effects on high-speed rotordynamics", Doctoral Thesis, University of Twente, Enschede, Netherlands.
- [4] Bulatovic, R. M., 1999, "A stability theorem for gyroscopic systems", Acta Mechanica, 136, pp. 119-124.
- [5] Chen, T. Y., and Wang, B. P., 1993, "Optimum design of rotor-bearing system with eigenvalue constraints", Journal of Engineering for Gas Turbines and Power, 115, pp. 256-260.
- [6] Jeffcott, H., 1919, "The lateral vibration of loaded shafts in the neighbourhood of a whirling speed-the effect of want of balance", Phil. Mag., 37 (6), pp. 304-314.
- [7] Nelson, H. D. and McVaugh, J. N., 1976, "The dynamics of rotor-bearing system using finite elements", Journal of Engineering for Industry, 98, pp. 593-600.
- [8] E.Kramer, Dynamics of Rotors and Foundations, Springer
- [9] A.S.Sekhar, Crack identification in a rotor system : a model based approach, Journal of Sound and Vibration 270(2004)887-902.
- [10] Shaft, Power Transmission, Aircraft Accessory, General Specification for Military Uses MIL-S-7470A, Dec. 9, 1975.